# Reactive oxygen and iron species monitoring to investigate the electro-Fenton performances. Impact of the electrochemical process on the biodegradability of metronidazole and its by-products

A. Abou Dalle, F. Fourcade, A.A. Assadi, L. Domergue, Hayet Djelal, T. Lendormi, S. Taha, A. Amrane

1 **Reactive oxygen and iron species monitoring to investigate the electro-**

2 **Fenton performances. Impact of the electrochemical process on the**

3 **biodegradability of metronidazole and its by-products.**

4 **Arwa ABOUDALLE[a,b], Florence FOURCADE[a*], Aymen Amin ASSADI[a], Lionel DOMERGUE[a],**

5 **Hayet DJELAL[a,d], Thomas LENDORMI[e] ,Samir TAHA[b,c] , Abdeltif AMRANE[a]**

a. *Univ rennes, Ecole Nationale Supérieure de Chimie de Rennes, CNRS, ISCR – UMR6226, F-35000 rennes, France*

b. *Laboratoire de Biotechnologies Appliquées, Centre AZM pour la recherche en biotechnologies et ses applications, Ecole doctorale des sciences et technologies, Université Libanaise, Rue Al-Mitein, Tripoli, Liban.*

c. *Faculté de Santé Publique, Université Libanaise, quartier Dam et Farz, Tripoli, Liban.*

d. *Ecole des Métiers de l'Environnement, Campus de Ker Lann, 35170 Bruz, France*

e. *Université Bretagne Sud, FRE CNRS 3744, IRDL, F-56300 Pontivy, France*

12

## 13 Abstract

14 In this study, the monitoring of reactive oxygen species and the regeneration of the ferrous

15 ions catalyst were performed during electro-Fenton (EF) process to highlight the influence of

16 operating parameters. The removal of metronidazole (MTZ) was implemented in an

17 electrochemical mono-compartment batch reactor under various ranges of current densities,

18 initial MTZ and ferrous ions concentrations, and pH values. It was found that under 0.07 mA

19 $cm^{-2}$, 0.1 mM of ferrous ions and pH=3, the efficiency of 100 mg $L^{-1}$ MTZ degradation and

20 mineralization were 100 % within 20 min and 40% within 135 min of electrolysis,

21 respectively. The highest hydrogen peroxide and hydroxyl radical concentrations, 1.4 mM and

22 2.28 mM respectively, were obtained at 60 min electrolysis at 0.07 mA $cm^{-2}$. Improvement of

23 the biodegradability was reached from 60 min of electrolysis with a $BOD_5/COD$ ratio above

24 0.4, which was reinforced by a respirometric study, that supports the feasibility of coupling

25 electro-Fenton and biological treatment for the metronidazole removal.

26

29

30    **1. Introduction**

31    Metronidazole (MTZ, 2-methyl-5-nitroimidazole-1-ethanol) is a nitroimidazole antibiotic, that

32    presents antibacterial and anti-inflammatory properties. MTZ is extensively used in Europe

33    for the treatment of infectious diseases caused by a wide range of anaerobic bacteria and

34    various protozoans, such as *Trichomonas vaginalis* and *Giardia lamblia* (Tally and Sullivan,

35    1981; Lau et al., 1992).

36    Because of its refractory character and a high solubility in water, MTZ is difficult to remove

37    during conventional sewage treatment (Kümmerer, 2001). Biorecalcitrance of this compound

38    was also demonstrated during culture of *Trametes Versicolor* fungus or using enzyme extract

39    from this fungus (Becker et al., 2016). As a result, MTZ accumulates in animals' body, fish-

40    farm waters and, more importantly, effluents from meat industries and hospitals (Kümmerer,

41    2001). Residual concentrations have consequently been detected in hospital effluents,

42    wastewater, surface water and groundwater (Dantas et al., 2010; Vulliet and Cren-Olivé,

43    2011). The results spotted that untreated release of MTZ exposes humans' health at risk

44    because of its potentially carcinogenic and mutagenic properties (Bendesky et al., 2002), its

45    toxicity against aquatic organisms (Lanzky and Halting-Sørensen, 1997) and genotoxicity to

46    humans since it causes a DNA damage in human lymphocytes (Ré et al., 1997).

47    Physico-chemical processes such as adsorption or ozonation can be performed to remove

48    refractory pharmaceutical pollutants in aqueous effluent including MTZ. Indeed, in their study

49    on MTZ adsorption, Rivera-Utrilla et al tested three different activated carbons. Results

50    showed the high adsorption capacity of the different activated carbons. Adsorption

51    phenomenon was more influenced by the activated carbons chemical properties rather than

52    their structural properties. Moreover, pH and the electrolyte concentration had a little

53    influence in the adsorption process, indicating a minor role of the electrostatic interactions

54    between MTZ and the activated carbons (Rivera-Utrilla et al., 2009). Adsorption is an

55    efficient process for MTZ removal but not destructive and then needs further post-treatment to

56    eliminate completely the pollutant.

57    Sánchez-Polo et al studied the removal of four different nitroimidazoles by ozonation process.

58    Low reactivity of nitroimidazoles with ozone was obtained with specific rate constants below

59    350 $M^{-1}$ $s^{-1}$ and only 10-20% of organic carbon reduction (Sánchez-Polo et al., 2008).

60    Among physico-chemical processes, Advanced Oxidation Processes (AOPs) are considered as

61    promising technologies for water remediation, based on the *in-situ* generation of strong

62    oxidants such as hydroxyl radical that react non-selectively with most persistent organic

63    pollutants in aqueous solutions until they reach total mineralization (conversion into $CO_2$,

64    water and inorganic ions) (Latimer, 1952; Ku et al., 1999; Stasinakis, 2008; Brillas et al.,

65    2009).

66    Several AOPs were tested by Shemer and his co-workers (Shemer et al., 2006). They found

67    that the degradation of metronidazole by photolysis was low; the concentration decrease was

68    around 10% over a period of 5 min. The addition of $H_2O_2$ to the UV irradiation improved the

69    efficiency of the degradation and the best degradation yield reached 67% for the same

70    duration. On other way, during Fenton's process, the metronidazole degradation yield i.e the

71    concentration decrease was enhanced to 76% (Shemer et al., 2006). This process is well

72    known as one of the most efficient AOPs (Lopez et al., 2004). Its implementation and

73    maintenance are simple since that needs only hydrogen peroxide and ferrous ions (Eq. 1)

74    (Lopez et al., 2004; Lu et al., 2005; Pignatello et al., 2006). It had been widely applied for the

75    treatment and pre-treatment of wastewater (Trujillo et al., 2006).

76    $H_2O_2 + Fe^{2+} \rightarrow Fe^{3+} + OH^- + \ ^{\cdot}OH$                                            (1)

77  When UV irradiation was applied in addition to the Fenton's reaction, quasi-total

78  metronidazole degradation was obtained (over 90%)(Shemer et al., 2006). Solar photo-Fenton

79  (Ammar et al., 2016) was also studied for the removal of metronidazole and based on COD

80  degradation, oxidation yield reached 96%.

81  Some studies based on the electro-Fenton process were carried out for the degradation of

82  metronidazole (Cheng et al., 2013; Pérez et al., 2015). This process is a combination of the

83  classical Fenton treatment with electrochemical reactions. It is based on the *in-situ* generation

84  of $H_2O_2$, brought by the continuous electrochemical reduction of dissolved oxygen as shown

85  in Eq. 2. Hydrogen peroxide reacts then with ferrous ions in catalytic amount to produce

86  hydroxyl radicals (Eq. 1) and ferrous ions were regenerated by their reduction at the cathode

87  surface. (Eq. 3) (Brillas et al., 2009).

88  $O_2 + 2H^+ + 2e^- \leftrightarrow H_2O_2$                                              (2)

89  $Fe^{3+} + e^- \leftrightarrow Fe^{2+}$                                                   (3)

90  Mineralization yield obtained with electro-Fenton did not exceed 40% in each study, and

91  increased to 53% with additional solar irradiation (Pérez et al., 2015).

92  For process intensification purpose in terms of mineralization, an alternative for the MTZ

93  removal was proposed. It concerned the improvement of biodegradability by the electro-

94  Fenton process prior to a subsequent biological mineralization (Mansour et al., 2012; Ferrag-

95  Siagh et al., 2014; Annabi et al., 2016; Olvera-Vargas et al., 2016; Ganzenko et al., 2017).

96  The interest of coupling physico-chemical process and biodegradation was already

97  highlighted (Scott and Ollis, 1995). In their study, the authors explained that the processes

98  order depends on the nature of the effluent to be treated. In presence of wastewater

99  concentrated in biorecalcitrant compounds, a chemical oxidation is required in order to

100 produce biodegradable by-products that will be then metabolized during the biological

101 process. Two sequences for the combination between electro-Fenton and biodegradation were

102  discussed for the removal of both 5-fluorouracil and caffeine at 0.1 mM (Ganzenko et al.,

103  2017). Both sequences were efficient for the removal of organic compounds. Biological pre-

104  treatment performances in a SBR reactor depended on microbial acclimation time and

105  biomass concentration. Residual organic load was then removed by electro-Fenton but a part

106  of the produced hydroxyl radicals was loss due to their attack on microorganism. During the

107  pre-pretreatment, pollutant biosorption could occur (Fontmorin et al., 2013) but was not

108  considered in this study. Moreover, the concentration of pollutants has an influence of the

109  biological treatment since for concentration higher than their inhibitory threshold for

110  microorganisms; biodegradation could be less efficient (Yahiat et al., 2011). When electro-

111  Fenton was performed as pre-treatment, biodegradability was improved by increasing the

112  electrolysis time and the current intensity. However, regarding the economic feasibility of the

113  electrochemical pre-treatment, long electrolysis duration with a low current intensity was a

114  better option.

115  An increase of the $BOD_5$/COD ratio was obtained after the MTZ electro-Fenton treatment

116  (Cheng et al., 2013), but below the limit of biodegradability (Alonso Salles et al., 2010).

117  In this study, in order to reach the limit of biodegradability, the influence of some operating

118  parameters was considered in regard to the production and the monitoring of reactive oxygen

119  species (hydrogen peroxide, hydroxyl radicals) and in regard to the behavior of iron species in

120  solution during electrolysis. The electrochemical behavior of metronidazole was also

121  examined in order to understand its rule in the compound degradation and mineralization.

122  Moreover, the estimation of biodegradability by means of the $BOD_5$/COD ration was

123  supported by a respirometric study implemented during 21 d.

124

125  **2. Materials and methods**

126  **2.1. Chemicals and materials**

5

127   MTZ (2-methyl-5-nitroimidazole-1-ethanol) with 99% of purity was purchased from Sigma-

128   Aldrich (Saint-Quentin Fallavier, France). $FeSO_4 \cdot 7H_2O$ (purity 99%) and $Na_2SO_4$ (purity

129   99%) were used as a catalyst source and inert supporting electrolyte respectively, and were

130   obtained from Acros Organics (Thermo Fisher Scientific, Geel, Belgium). Acetonitrile (purity

131   99.9%) (HPLC grade) was also obtained from Sigma–Aldrich. All solutions were prepared

132   with ultrapure water and all other chemicals used for analysis were purchased from Acros and

133   Sigma.

134   **2.2. Electrochemical Apparatus and Procedures**

135   Experiments were performed at ambient temperature (20°C) in a discontinuous reactor

136   containing 250 mL of solution and were previously detailed (Abou Dalle et al., 2017). An

137   ammeter power supply (Microsonic systems, Microlab MX 20V-2A, France) delivered

138   cathodic current intensity throughout the electrolysis between two electrodes. A tri-

139   dimensional piece of graphite felt of 42 $cm^3$ geometrical volume was used as cathode (Le

140   Carbone Lorraine RVG 4000 Mersen, Paris la Défense, France) and the anode was a platinum

141   cylinder (32 $cm^2$ ). Compressed air was bubbled into the solution for 10 min before the

142   electrolysis to saturate the solution with $O_2$ and then throughout the experiments.

143   $FeSO_4 \cdot 7H_2O$ was added into the cell just before the beginning of the electrolysis. 50 mM

144   $Na_2SO_4$ was added as supporting electrolyte.

145

146   **2.3Analytical procedure**

147   **2.3.1. Electrochemical analysis**

148   Current-potential curves were performed in a conventional three electrodes electrochemical

149   cell as previously detailed (Fourcade et al., 2013). The electrochemical apparatus was a

150   SP150 BioLogic potentiostat/galvanostat (BioLogic SAS, Clais, France) with EC-Lab[®]

151   software.

**2.3.2. High Performance Liquid Chromatography (HPLC).**

The degradation of Metronidazole was measured by HPLC using Waters 996 system equipped with Waters 996 PDA (Photodiode Array Detector) and Waters 600LCD Pump. The separation was achieved on Waters C 18 (5 μm; $4.6 \times 250$ mm) reversed-phase. The eluent consisted of an acetonitrile/water mixture (20/80, v/v) with 0.1% formic acid delivered at a flow rate of 1 mL min$^{-1}$. The detection of Metronidazole was carried out at 318 nm and the retention time was 4.3 min.

**2.3.3. Total organic carbon (TOC) measurement.**

TOC was measured by TOC-V$_{CPH/CPG}$ Total Organic Analyzer Schimadzu. $CO_2$ produced from the combustion and the conversion of Organic Carbon compounds was identified by non-dispersive Infra-Red Detector (NDIR).

**2.3.4. Hydrogen peroxide quantification.**

Hydrogen peroxide concentration was iodometrically measured with sodium thiosulfate as titrant, by amperometric titration with a double Pt indicator electrode and an applied potential difference of 100 mV (Potentio-amperometric TPA4 titrator, Tacussel, Lyon, France) (Abou Dalle et al., 2017).

**2.3.5. Hydroxyl radical's quantification**

Dimethyl sulfoxide (DMSO) was used to trap hydroxyl radicals (Abou Dalle et al., 2017). It reacts quickly with a hydroxyl radical forming methanesulfonic acid and sulfate (Jahnke, 1999). DIONEX DX120 ion chromatography was used to detect the formed methanesulfonic acid. A DIONEX DX120 chromatograph was provided with a conductivity detector; the stationary phase is constituted by an anion exchange column AS19 (4 x 250 mm) and the mobile phase was constituted of a KOH solution in water. A gradient elution mode was adopted for the analyses. 10 mM of KOH was considered during the first 10 min; then the amount increased linearly to reach 45 mM from 10 to 25 min; and finally an amount of 45

177  mM of KOH was maintained from 25 to 35 min of the analysis. The flow rate remained

178  constant at 1 mL min$^{-1}$.

179  **2.3.6. Iron species quantification.**

180  Total dissolved iron species were quantified by atomic absorption spectrometry (AA140,

181  VARIAN spectrometer, Palo Alto, USA) with air/acetylene flame at 372 nm. Ferrous ions

182  were quantified by the orthophenanthroline complexometric method, detailed in a previous

183  work (Ben Hammouda et al., 2016).

184  **2.3.7. Biochemical oxygen demand (BOD$_5$) measurements**

185  The inoculated activated sludge was obtained from a municipal wastewater treatment plant

186  (Beaurade, Rennes, France).The activated sludge was cultivated under oxygen flow on a

187  previously detailed mineral medium (Fontmorin et al., 2012). Before inoculation, the

188  activated sludge was washed three times with tap water and twice with ultrapure water to

189  remove all carbon residues. A verification of the elimination of these latter was carried out by

190  analyzing the TOC values.

191  BOD$_5$ measurements were carried out in Oxitop IS6 (WTW, Alès, France) under a previously

192  detailed protocol (Fontmorin et al., 2012).

193  **2.3.8. Respirometric experiments**

194  Experiments were carried out in 3L bioreactor (Bioflow 3000, New Brunswick scientific)

195  coupled to a respirometric device measuring Oxygen Uptake Rates (OUR) of activated sludge

196  (Spérandio and Paul, 2000; Adouani et al., 2015). This latter was collected from the biological

197  basin of Pontivy (Brittany, France) Waste Water Treatment Plant.

198  2.5 L of settled sludge, after sifting at 400 μm, were aerated in the bioreactor; pH and

199  temperature were controlled to 7.7 and 25°C respectively. Dissolved oxygen uptake rate was

200  measured continuously in the bioreactor. Biological activity of heterotrophic biomass can be

201  then characterized as well as its behavior (a possible microorganism's inhibition for example)

8

202  in the presence of 500 mg L$^{-1}$ MTZ or its electrolyzed solutions. First, endogenous respiration

203  was measured (OUR$_{endo}$). To characterize heterotrophic biomass activity, a biodegradable

204  carbon source, here sodium acetate (0.1 g), was firstly added in the culture medium when

205  OUR$_{endo}$ was stable and exogenous respiration (OUR)$_{exo}$ was measured. MTZ or electrolyzed

206  solution was then added to reach TOC values in the range 5-50 mg C L$^{-1}$ in the bioreactor.

207  When the OUR$_{endo}$ remained stable, sodium acetate was added again, the response of OUR$_{exo}$

208  was compared with the previous one. To characterize autotrophic biomass activity, sodium

209  acetate was replaced by a mineral substrate (NH$_4$Cl 0.1 g). These tests were performed during

210  21 d. The analysis of the different curve patterns (OUR function of time) provided

211  information on the metabolization of each substrate.
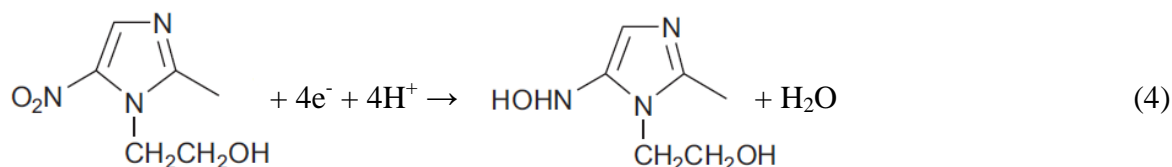
212

213  **3. Results and discussion**

214  **3.1. Evolution of MTZ degradation and mineralization**

215  Metronidazole degradation and mineralization were first studied during electrolysis at 0.04

216  mA cm$^{-2}$ in a 50 mM sodium sulfate solution at pH 3 with 0.1 mM of ferrous ions and for an

217  initial concentration of 100 mg L$^{-1}$. The degradation kinetic was rapid compared to the

218  mineralization kinetic since an almost total degradation of the target compound was obtained

219  at 25 min. After 135 min of electrolysis, mineralization yield was only 26% (Fig 1a). The

220  recalcitrance of metronidazole by-products during electro-Fenton treatment was already

221  noticed by Pérez et al. (Pérez et al., 2015) and could explain the moderate mineralization yield

222  obtained. In their study, the identified heterocyclic by-products included an imidazole ring

223  that is considered as stable because of the presence of two nitrogen atoms in the aromatic

224  cycle. In the imidazole ring, a free electron doublet associated to the pyrrole nitrogen is

225  delocalized in the cycle and electrons from pyridine nitrogen are localized in its sp$^2$ orbital.

226  This particular configuration confers stability to the imidazole ring (Clayden et al., 2002) and

9

227 could then confer its recalcitrance toward hydroxyl radical attack. In the same way, cyanuric

228 acide is well known as recalcitrant to hydroxyl radical oxidation due to the electron deficiency

229 of the triazine ring linked to the higher electronegativity of nitrogen compared to that of

230 carbon (Liu, 2014).

231 Different evolutions for MTZ concentration during electrolysis conducted at 0.07 mA cm$^{-2}$

232 with 0.1 mM of ferrous ions were plotted according to the initial target compound

233 concentration in the range of 100-500 mg L$^{-1}$ (Fig. SM-1). As almost total degradation was

234 obtained after 20 min for 100 mg L$^{-1}$ MTZ initial concentration, the time needed for a total

235 degradation increased to 30 min doubling the initial concentration. If we considered a pseudo

236 first order kinetic for the global degradation as mentioned in most of the studies on the

237 electro-Fenton process (Brillas et al., 2009), apparent initial kinetic constant ($k_{app}$) deduced

238 from the 10 first min of electrolysis (Table 1) highlighted a higher reaction kinetic for an

239 initial concentration of 100 mg L$^{-1}$. Then $k_{app}$ decreased with the initial MTZ concentration.

240 These results were in accordance with previous studies (Ferrag-Siagh et al., 2014; Annabi et

241 al., 2016) and can be explained by a gradual acceleration of competitive reactions between the

242 degradation of the target compound and that of its by-products.

243 The electrochemical behavior of metronidazole was also studied in order to study the

244 contribution of a direct oxidation and/or reduction of the target molecule at the electrode

245 surface during the electro-Fenton process. For this purpose, current potential curves were

246 plotted with a vitreous carbon rotating disk electrode in $Na_2SO_4$ 50 mM supporting electrolyte

247 at pH 3 with 100 mg L$^{-1}$ of the target compound and under nitrogen atmosphere. No MTZ

248 oxidation was highlighted (data not show) while a signal for MTZ reduction was observed

249 around - 0.4 V/SCE (Fig. 1b). The MTZ electrochemical reaction was already highlighted by

250 Saïdi et al. (Saïdi et al., 2014) in acidic aqueous medium $H_2SO_4$ (0.5 M) and corresponded to

251 the four-electrons reduction of the nitro group to the corresponding hydroxylamine (Eq. 4).

252

253 $O_2N$ ⎯⎯ (imidazole ring) $N$⎯$CH_3$, $CH_2CH_2OH$ $+ 4e^- + 4H^+ \rightarrow$ $HOHN$ ⎯⎯ (imidazole ring) $N$⎯$CH_3$, $CH_2CH_2OH$ $+ H_2O$     (4)

254

255 During MTZ electrolysis in the same operating conditions as for electro-Fenton but in the

256 presence of tert-butanol, well-known as an hydroxyl radical's scavenger (Ma and Graham,

257 2000), kinetic of MTZ degradation was slower since an almost total degradation was obtained

258 for around 40 min (not shown) compared to 25 min for electrolysis without tert-butanol. The

259 electric charge (Q) was calculated using the Faraday's law (Eq. 5) with F the Faraday

260 constant, N the mol number of degraded MTZ and n the 4 electrons reduction of

261 metronidazole. According to the consumed electric charge during 40 min of electrolysis in the

262 presence of tert-butanol (Eq. 6), the current efficiency was about 47%.

263 $Q = n\,F\,N$     (5)

264 $Q = i\,t$     (6)

265 It can be therefore supposed that metronidazole degradation was due to both the

266 electrochemical reduction at the cathode surface and the oxidation by hydroxyl radicals.

267 Under nitrogen atmosphere to avoid the presence of oxygen in the solution and then the

268 production of hydrogen peroxide, mineralization yield was negligible (not shown). This result

269 confirms that metronidazole mineralization was mainly due to the action of hydroxyl radicals

270 produced by the Fenton reaction.

271

272 **3.2. Effect of the applied cathodic current density**

273 **3.2.1. Effect of the applied cathodic current density on MTZ degradation and mineralization**

274 Current density is one of the main parameters governing the efficiency of the electro-Fenton

275 process, governing the formation of $H_2O_2$ and then that of hydroxyl radicals (Oturan et al.,

276 2008; Özcan et al., 2009; Feng et al., 2014). Cathodic current density affects the organic

277     matter treatment performance (Brillas et al., 2000). Its impact on the degradation and the

278     mineralization of MTZ was therefore examined. The figure 2a shows the evolution of

279     metronidazole concentration as a function of time for different cathodic current densities

280     ranging from 0.04 to 0.45 mA cm$^{-2}$. The obtained results showed an almost total degradation

281     except for 0.04 mA cm$^{-2}$ after 15 min of electrolysis (Fig. 2a). In the range 0.07 to 0.22 mA

282     cm$^{-2}$, the $k_{app}$ were nearly similar, in a short range of values, 0.22 to 0.24 min$^{-1}$ (Table 1),

283     while for 0.04 mA cm$^{-2}$, the apparent constant kinetics was lows, about 0.08 min$^{-1}$. The weak

284     maximum value observed for 0.07 mA cm$^{-2}$ should however be noticed.

285     This faster oxidation at 0.07 mA cm$^{-2}$ can be ascribed to an acceleration of the $H_2O_2$

286     formation rate according to reaction (Eq. 2) and was confirmed by the hydrogen peroxide

287     quantification (Fig. 3b). A good regeneration of ferrous ions from reaction (Eq. 3), as

288     mentioned in paragraph 3.2.2., can also explain the better efficiency of the electro-Fenton

289     process at 0.07 mA cm$^{-2}$ if compared to higher current densities (Brillas et al., 2009). At

290     higher current densities, the production of hydrogen peroxide was lower (Fig. 3b).

291     As observed in Fig. 3a, plotting the concentration decrease according to the electric charge

292     (Q) highlighted the presence of competitive reactions since the necessary electric charge for a

293     total degradation increased with the current density. At 0.07 mA cm$^{-2}$, total degradation was

294     obtained for an electric charge of 120 C. When current density increased to 0.45 mA cm$^{-2}$

295     total MTZ degradation required more than 600 C. Concurrent reactions such as the direct 4

296     electrons oxygen reduction (Eq. 7), hydrogen peroxide reduction (Eq. 8) or formation of

297     hydrogen (Eq. 9) at the cathode and the oxidation of $H_2O_2$ on the anode (Eq.10) in the

298     undivided cell can impede the accumulation of hydrogen peroxide (Brillas et al., 2009; Dirany

299     et al., 2012; Ferrag-Siagh et al., 2013). Because of these competing reactions, the constant

300     rate $k_{app}$ (Table 1) cannot be proportional to the current density (Annabi et al., 2016).

301     $$O_2 + 4H^+\ 4e^- \rightarrow \quad 2H_2O \tag{7}$$

302     $H_2O_2 + 2H^+ + 2e^- \quad \rightarrow \quad 2H_2O$                      (8)

303     $2H_3O^+ + 2e^- \quad \rightarrow \quad H_2 + 2H_2O$                      (9)

304     $H_2O_2 \quad \rightarrow \quad O_2 + 2e^- + 2H^+$                        (10)

305

306     Mineralization yields remained limited irrespective of the applied current density (Fig. 2b)

307     due to the recalcitrance of metronidazole by-products as mentioned before. For instance, for a

308     current density of 0.04 mA cm$^{-2}$, the TOC removal was only 26 % after 135 min of treatment.

309     TOC removal increased to 40 % with a current density of 0.07 mA cm$^{-2}$. This highest

310     mineralization yield was also in accordance with the highest concentration of hydrogen

311     peroxide obtained, 1.4 mM (Fig. 3b); while a lower production of hydrogen peroxide was

312     observed for a further increase of the current density.

313

314     **3.2.2. Effect of the current density on the concentration of iron species.**

315     The evolution of the ferrous and ferric ions concentrations in the solution during the electro-

316     Fenton process at different current densities is presented in Fig. 4a.  The total concentration of

317     iron ions remained constant throughout the electrolysis for 0.04 mA cm$^{-2}$; while a decrease of

318     this concentration of about 15% was observed when the current density increased to 0.07 mA

319     cm$^{-2}$. For 0.22 and 0.45 mA cm$^{-2}$, an almost total disappearance of the total iron ions in

320     solution was observed from 60 min of electrolysis. Indeed, for high current densities, water

321     reduction can lead to a local alkalinization of the solution caused by hydroxyl anions

322     formation during $H_2$ release and then to the precipitation of iron as $Fe(OH)_3$ (Eq. 11) (Brillas

323     et al., 2009; Petrucci et al., 2016).

324     $2H_2O + 2e^- \leftrightarrow H_{2\,(g)} + 2OH^-$                         (11)

325  The adsorption of iron hydroxide onto the electrode surface (Petrucci et al., 2016) or the

326  reduction of iron ions to metallic iron considering standard potentials for iron redox couples,

327  could be checked even if no deposit on the electrode surface was observed after electrolysis.

328  All these phenomena could then partly explain a lower efficiency for these current densities.

329  In order to study the regeneration of ferrous ions, electrolysis at 0.04 and 0.07 mA cm$^{-2}$ were

330  carried out under $N_2$ inert atmosphere, in order to avoid dissolved $O_2$ and then the electro-

331  generation of $H_2O_2$ (Fig. 4b). An initial amount of ferric ions of 0.1 mM was added into the

332  reactor at pH 3. At the initial time, without electrodes polarization, the slight amount of

333  ferrous ions detected can be explained by redox equilibrium between ferrous and ferric ions in

334  solution. Since the electrodes polarization, ferrous ions were detected very quickly in solution

335  at a value of 0.06 mM for both current densities, and remained then stable throughout

336  electrolysis. 60% of ferric ions were reduced at the cathode surface and as the concentration

337  of total iron ions in solution remained quasi constant in solution, 40% of ferric ions remained

338  in solution; this could be explained by an equilibrium between ferrous and ferric ions

339  implemented in solution throughout the electrolysis. In addition, the evolution of ferrous ions

340  generation was similar for both current intensities, as for the total concentration of iron

341  species. The difference observed between 0.04 and 0.07 mA cm$^{-2}$ concerning mineralization

342  can be then explained by the higher production of hydrogen peroxide measured for the latter

343  current density.

344

345  **3.3. Influence of the initial catalyst concentration**

346  In order to evaluate the effect of the catalyst concentration on the degradation and the

347  mineralization of Metronidazole, several experiments were performed in the presence of 100

348  mg L$^{-1}$ of MTZ at pH 3 and an applied current density of 0.07 mA cm$^{-2}$. The degradation of

349  the target compound was slighthly influenced by the concentration of ferrous ions in the

350  studied range from 0.05 to 1 mM (Fig. SM-2). Indeed, for 15 min of electrolysis, degradation

351  yields were in a short range of values, 90 to 99% with a slight peak (99%) for 0.1 mM of

352  catalyst. Because of the electrochemical reduction of metronidazole at the cathode surface and

353  a good regeneration of ferrous ions at these current densities, the influence of the ferrous ions

354  amount on the metronidazole degradation can be considered as low in this range of

355  concentrations. MTZ mineralization also showed a slight peak in the range of catalyst

356  concentrations tested; it increased from 20% to 32% at 120 min of electrolysis for increasing

357  $Fe^{2+}$concentrations from 0.05 to 0.1 mM respectively (Fig. SM-2). This increase could be

358  attributed to the increase of the production of hydroxyl radicals from 1.52 to 2.28 mM

359  respectively (Table 2). The MTZ mineralization and the production of hydroxyl radicals

360  remained then constant for 0.5 mM and then decreased for 1 mM of ferrous ions. For this

361  latter ferrous concentration, mineralization yield was 23% after 120 min and the concentration

362  of produced hydroxyl radical decreased to 1.56 mM for 60 min of electrolysis respectively

363  (Fig. SM-2 and Table 2). This decrease can be explained by competition effects between

364  hydroxyl radicals resulting from the Fenton's reaction and the excess of ferrous ions (Panizza

365  and Cerisola, 2009), according to Eq. 12.

366  $Fe^{2+} + {}^{\bullet}OH \leftrightarrow Fe^{3+} + OH^{-}$ (12)

367  It can be therefore deduced that the optimal value for ferrous ions was 0.1 mM. This value

368  was in accordance with other studies, such as the mineralization by the electro-Fenton process

369  of tetracycline (Ferrag-Siagh et al., 2013) , direct orange 61 (Hammami et al., 2007) and

370  pentachlorophenol (Oturan et al., 2001). However, the influence of this parameter is not

371  essential in this range of concentrations since the difference between the mineralization yields

372  for all tested ferrous ions concentrations did not exceed 12%.

373

374

### 3.4. Effect of the pH

To consider the effect of pH on the electro-Fenton process, degradation and mineralization of MTZ were studied at different pH values from 2 to 9. The degradation of metronidazole was achieved by the Fenton's reaction and such reaction is highly related to the pH (Brillas et al., 2009). Moreover, it was also shown that the electrochemical reduction of metronidazole depends also on the pH (Saïdi et al., 2014), in agreement with the impact of the pH on the degradation rate of metronidazole experimentally observed (Table 1). Indeed, for acidic media, values of $k_{app}$ (0.18 and 0.17 min$^{-1}$ for pH 2 and 3 respectively) were higher compared to those obtained in neutral and basic media (0.08, 0.08, 0.05 min$^{-1}$ for pH 5, 7 and 9 respectively). The mineralization yields decreased from 32% to 24% after 120 min when pH decreased from 3 to 2 respectively (Fig. SM-3). At higher pH values, the degradation of metronidazole was very slow (Fig. SM-3) and reached 83.0%, 80.7%, 65.4% after 30 min, while mineralization yields were 17.0%, 8.3%, and 5.9% after 2 hours for pH 5, pH 7 and pH 9 respectively. Optimal mineralization yield (32%) was obtained at pH 3. Higher amounts of hydroxyl radicals were obtained at acidic pH (Table 2) and the optimal production of hydroxyl radicals was reached at pH 3, that is consistent with the related literature (Qiang et al., 2003; Ramirez et al., 2005; Zhou et al., 2007; Ramirez et al., 2009). At pH values lower than 3, ferric ions can form complexes with hydrogen peroxide leading to lower production of hydroxyl radicals (1.95 ± 0.09 mM – Table 2). Moreover, The $H_2$ evolution can be favored at acidic pH (Petrucci et al., 2016) and hydrogen peroxide would form an oxonium ion (Eq. 13) which inhibits the formation of hydroxyl radicals (Sun et al., 2009; Zhou et al., 2013). For higher values of pH, the precipitation of ferric ions (Eq. 14) and then a lower production of hydroxyl radicals (Table 2) leads to a loss of efficiency (Brillas et al., 2009; Masomboon et al., 2009; Nidheesh and Gandhimathi, 2012).

$$H_2O_2 + H^+ \leftrightarrow H_3O_2^+ \tag{13}$$

400    $Fe^{3+} + 3OH^- \leftrightarrow Fe(OH)_3$                                                                    (14)

401

402    **4. Biodegradability of the electrolyzed solution of MTZ**

403    Once the solution was treated by electro-Fenton, since organic carbon was still present in

404    solution due to low mineralization yield, a combined process involving a subsequent

405    biological treatment could be considered in order to complete the mineralization of the

406    electrolyzed solution. To assess the relevance of such combined process, the biodegradability

407    should be first determined, it corresponded to the $BOD_5$ on COD ratio; a solution is

408    considered as easily biodegradable from a ratio of 0.4 (Alonso Salles et al., 2010).

409    Table 3 reported the time-course of the ratio values of 100 mg $L^{-1}$ MTZ electrolysis at 0.07

410    mA $cm^{-2}$ and with 0.1 mM of ferrous ions. $BOD_5$ /COD ratio values suggested that the initial

411    MTZ solution was not biodegradable. After 30 min of electrolysis, even if a total degradation

412    of MTZ was observed (Fig. 1), the solution remained not biodegradable with a ratio of 0.24,

413    showing that the MTZ by-products, at this time of electrolysis, were relatively resistant to

414    micro-organisms since these components were structurally close to the target compound

415    (Mansour et al., 2012). However, the slight improvement of biodegradability can be due to

416    short linear aliphatic carboxylic acids resulting from the loss of lateral ethanol and acetic acid

417    group during the oxidation of MTZ and its heterocyclic intermediates (Pérez et al., 2015) that

418    can be metabolized by microorganisms. The solution became biodegradable since the ratio

419    value reached 0.7 for 120 min of electrolysis (Table 3). It can be therefore supposed that a

420    large part of recalcitrant by-products was oxidized beyond 60 min since the ratio reached 0.46

421    and can be therefore considered as an optimal oxidation time to minimize the energy

422    consumption. Respirometric experiments showed that no inhibition of heterotrophic and

423    autotrophic biomasses was observed whether after the injection of a non-electrolyzed solution

424    of MTZ or an electrolyzed one. Whereas no response in OUR curve was observed with a non-

425  electrolyzed solution of MTZ at the beginning of the test, direct response was observed with

426  the first injection of the electrolyzed solution of MTZ which supported the $BOD_5$ results (data

427  not show). Moreover, after 18 d, a response in OUR curve was observed with a non-

428  electrolyzed solution of MTZ (data not show), which would prove that biomass could be

429  acclimatized to MTZ and perform its direct degradation. The biodegradability improvement

430  after electro-Fenton treatment of recalcitrant compounds was also noticed in several reports

431  (Alonso Salles et al., 2010; Mansour et al., 2012; Ferrag-Siagh et al., 2014; Annabi et al.,

432  2016). Even if the respirometric study assumed a possible biodegradation of pure MTZ after

433  18 d, the electro-Fenton pretreatment should allow to significantly decrease the

434  biodegradation duration.

435  **4. Conclusion**

436  The degradation and mineralization of metronidazole was studied by the electro-Fenton

437  process in a mono-compartment discontinuous reactor including a carbon felt cathode and a

438  platinum anode. Both the MTZ electrochemical reduction at the cathode surface and the

439  Fenton reaction were responsible for the degradation of the target compound. However,

440  mineralization was mainly due to the production *in-situ* of hydroxyl radicals. The influence of

441  some operating parameters such as initial Metronidazole's concentration, current intensity,

442  initial $Fe^{2+}$ concentration, and pH value was examined. The highest generation of hydrogen

443  peroxide was obtained at 0.07 mA cm$^{-2}$ with a good regeneration of ferrous ions and at this

444  current density, production of hydroxyl radicals was the highest at pH 3 with 0.1 mM ferrous

445  ions. These conditions were considered as optimal and allowed a total degradation of MTZ

446  and 40% mineralization within 20 min and 135 min of electrolysis, respectively. Additionally,

447  an improvement of the biodegradability to 0.46 was reached from 60 min of electrolysis and

448  was supported by respirometry, indicating the relevance of the electro-Fenton process as a

449  pretreatment prior to a subsequent biological treatment to complete the mineralization.

450

**References**

Abou Dalle, A., Domergue, L., Fourcade, F., Assadi, A.A., Djelal, H., Lendormi, T., Soutrel, I., Taha, S., Amrane, A., 2017. Efficiency of DMSO as hydroxyl radical probe in an Electrochemical Advanced Oxidation Process – Reactive oxygen species monitoring and impact of the current density. Electrochim. Acta 246, 1-8.

Adouani, N., Limousy, L., Lendormi, T., Sires, O., 2015. $N_2O$ and NO emissions during wastewater denitrification step: Influence of temperature on the biological process. C.R. Chimie 18, 15-22.

Alonso Salles, N., Fourcade, F., Geneste, F., Floner, D., Amrane, A., 2010. Relevance of en electrochemical process prior to a biological treatment for the removal of an organophosphorous pesticide, phosmet. J. Hazard. Mater. 181, 617-623.

Ammar, H.B., Ben Brahim, M., Abdelhédi, R., Samet, Y., 2016. Enhanced degradation of metronidazole by sunlight via photo-Fenton process under gradual addition of hydrogen peroxide. J. Mol. Catal. A.-Chem. 420, 222-227.

Annabi, C., Fourcade, F., Soutrel, I., Geneste, F., Floner, D., N., B., Amrane, A., 2016. Degradation of enoxacin by the electro-Fenton process: optimization, biodegradability improvement and degradation mechanism. J. Environ. Manage. 165, 96-105.

Becker, D., Della Giustina, S.V., Rodriguez-Mozaz, S., Schoevaart, R., Barceló, D., De Cazes, M., Belleville, M.P., Sanchez-Marcano, J., De Gunzburg, J., Couillerot, O., Völker, J., Oehlmann, J., Wagner, M., 2016. Removal of antibiotics in wastewater by enzymatic treatment with fungal laccase – Degradation of compounds does not always eliminate toxicity. Bioresource Technol. 219, 500-509.

Ben Hammouda, S., Fourcade, F., Assadi, A., Soutrel, I., Adhoum, N., Monser, L., Amrane, A., 2016. Effective heterogeneous electro-Fenton process for the degradation of a malodorous compound, indole, using iron loaded alginate beads as a reusable catalyst. Appl. Catal. B-Environ. 182, 47-58.

Bendesky, A., Menéndez, D., Ostrosky-Wegman, P., 2002. Is metronidazole carcinogenic? Mutat. Res- Rev. Mutat. 511, 133-144.

Brillas, E., Calpe, J.C., Casado, J., 2000. Mineralization of 2,4-D by advanced electrochemical oxidation processes. Water Res. 34, 2253-2262.

Brillas, E., Sirés, I., Oturan, M.A., 2009. Electro-Fenton process and related electrochemical technologies based on Fenton's reaction chemistry. Chem. Rev. 109, 6570-6631.

Cheng, W., Yang, M., Xie, Y., Liang, B., Fang, Z., Tsang, E.P., 2013. Enhancement of mineralization of metronidazole by the electro-Fenton process with a $Ce/SnO_2$-Sb coated titanium anode. Chem. Eng. J. 220, 214-220.

19

497 Clayden, J., Greeves, N., Warren, S., Wothers, P., 2002. Chimie Organique. First ed. De
498 Boeck, Paris.

499 Dantas, R.F., Rossiter, O., Teixera, A.K.R., Simões, A.S., Da Silva, V.L., 2010. Direct UV
500 photolysis of propanolol and metronidazole in aqueous solutions. Chem. Eng. J. 158, 143-
501 147.

502

503 Dirany, A., Sirés, I., Oturan, N., Özcan, A., Oturan, M.A., 2012. Electrochemical treatment of
504 the antibiotic sulfachloropyridazine: kinetics, reaction pathways and toxicity evolution.
505 Environ. Sci. Technol. 46, 4074-4082.

506

507 Feng, L., N., O., Van Hullebusch, E.D., Esposito, G., Oturan, M.A., 2014. Degradation of
508 anti-inflammatory drug ketoprofen by electro-oxidation: comparison of electro-Fenton and
509 anodic oxidation processes. Environ. Sci. Pollut. R. 21, 8406-8416.

510

511 Ferrag-Siagh, F., Fourcade, F., Soutrel, I., Aït-Amar, H., Djelal, H., Amrane, A., 2013.
512 Tetracycline degradation and mineralization by the coupling of an electro-Fenton
513 pretreatment and a biological process. J. Chem. Technol. Biot. 88, 1380-1386.

514

515 Ferrag-Siagh, F., Fourcade, F., Soutrel, I., Aït Amar, H., Djelal, H., Amrane, A., 2014.
516 Electro-Fenton pretreatment for the improvement of tylosin biodegradability. Environ. Sci.
517 Pollut. R. 21, 8534-8542.

518

519 Fontmorin, J.M., Fourcade, F., Geneste, F., Floner, D., Huguet, S., Amrane, A., 2013.
520 Combined process for 2,4-dichlorophenoxyacetic acid treatment - Coupling of an
521 electrochemical system with a biological treatment. Biochem. Eng. J. 70, 17-22.

522

523 Fontmorin, J.M., Huguet, S., Fourcade, F., Geneste, F., Floner, D., Amrane, A., 2012.
524 Electrochemical oxidation of 2,4-dichlorophenoxyacetic acid: analysis of by-products and
525 improvement of the biodegradability. Chem. Eng. J. 195-196, 208-217.

526

527 Fourcade, F., Delawarde, M., Guihard, L., Nicolas, S., Amrane, A., 2013. Electrochemical
528 reduction prior to electro-Fenton oxidation of azo dyes: Impact of the pretreatment on
529 biodegradability. Water Air Soil Poll. 224, 1-11.

530

531 Ganzenko, O., Trellu, C., Papirio, S., Oturan, N., Huguenot, D., Van Hullebusch, E.D.,
532 Esposito, G., Oturan, M.A., 2017. Bioelectro-Fenton: evaluation of a combined biological-
533 advanced oxidation treatment for pharmaceutical wastewater. Envir. Sci. Pollut. R. doi:
534 10.1007/s11356-017-8450-6.

535

536 Hammami, S., Oturan, N., Bellakhal, N., Dachraoui, M., Oturan, M.A., 2007. Oxidative
537 degradation of direct orange 61 by electro-Fenton process using a carbon felt electrode:
538 Application of the experimental design methodology. J. Electroanal. Chem. 610, 75-84.

539

540 Jahnke, L.S., 1999. Measurement of hydroxyl radical - generated methane sulfinic acid by
541 high-performance liquid chromatography and electrochemical detection. Anal. Biochem. 269,
542 273-277.

543

544 Ku, Y., Chen, K., Lee, K., 1999. Ultrasonic destruction of 2-chlorophenol in aqueous
545 solution. Water Res. 31, 929-935.

546

547 Kümmerer, K., 2001. Drugs in the environment: emission of drugs, diagnostic aids and
548 disinfectants into wastewater by hospital in relation to other sources - a review. Chemosphere
549 45, 957-969.
550
551 Lanzky, P.F., Halting-Sørensen, B., 1997. The toxic effect of the antibiotic metronidazole on
552 aquatic organisms. Chemosphere 35, 2553-2561.
553
554 Latimer, W.M., 1952. Oxidation potentials. Prentice Hall, New York.
555
556 Lau, A.H., Lam, N.P., Piscitelli, S.C., Wilkes, L., Danziger, L.H., 1992. Clinical
557 pharmacokinetics of metronidazole and other nitroimidazole anti-infectives. Clin.
558 Pharmacokinet. 23, 328-364.
559
560 Liu, G., 2014. Recalcitrance of cyanuric acid to oxidative degradation by OH radical:
561 theoretical investigation. RSC Adv. 4, 37359-37364.
562
563 Lopez, A., Pagano, M., Volpe, A., Di Pinto, A.C., 2004. Fenton's pre-treatment of mature
564 landfill leachate. Chemosphere 54, 1005-1010.
565
566 Lu, M.C., Zhang, H., Huang, Y.Y., Wang, S.Y., 2005. Influence of organic ions on the
567 mineralization of 2,4-dinitrophenol by the Fenton reaction. Fresen. Environ. Bull. 14, 101-
568 104.
569
570 Ma, J., Graham, N.J., 2000. Degradation of atrazine bu manganese-catalyzed ozonation -
571 influence of radical scavenger. Water Res. 34, 3822-3828.
572
573 Mansour, D., Fourcade, F., Bellakhal, N., Dachraoui, M., Hauchard, D., Amrane, A., 2012.
574 Biodegradability improvement of sulfamethazine solutions by means of electro-Fenton
575 Process. Water Air Soil Poll. 223, 2023-2034.
576
577 Masomboon, N., Ratanatamskul, C., Lu, M.C., 2009. Chemical oxidation of 2,6-
578 dimethylaniline in the Fenton process. Environ. Sci. Technol. 43, 8629-8634.
579
580 Nidheesh, P.V., Gandhimathi, R., 2012. Trends in electro-Fenton process for water and
581 wastewater treatment: An overview. Desalination 299, 1-15.
582
583 Olvera-Vargas, H., Cocerva, T., Oturan, N., Buisson, D., Oturan, M.A., 2016. Bioelectro-
584 Fenton: A sustainable integrated process for removal of organic pollutants from water:
585 Application to mineralization of metoprolol. J. Hazard. Mater. 319, 13-23.
586
587 Oturan, M.A., Oturan, N., Lahitte, C., Trevin, S., 2001. Production of hydroxyl radicals by
588 electrochemically assisted Fenton's reagent: application to the mineralization of an organic
589 micropollutant, pentachlorophenol. J. Electroanal. Chem. 507, 96-102.
590
591 Oturan, M.A., Pimentel, M., Otuan, N., Sirés, I., 2008. Reaction sequence for the
592 mineralization of the short-chain carboxylic acids usually formed upon cleavage of aromatics
593 during electrochemical Fenton treatment. Electrochim. Acta 54, 173-182.
594
595 Özcan, A., Oturan, M.A., Oturan, N., Sahin, Y., 2009. Removal of Acid Orange 7 from water
596 by electrochemically generated Fenton's reagent. J. Hazard. Mater. 163, 1213-1220.

Panizza, M., Cerisola, G., 2009. Electro-Fenton degradation of synthetic dyes. Water Res. 43, 339-344.

Pérez, T., Garcia-Segura, S., El-Ghenymy, A., Nava, J.L., Brillas, E., 2015. Solar photoelectro-Fenton degradation of the antibiotic metronidazole using a flow plant with a Pt/air-diffusion cell and a CPC photoreactor. Electrochim. Acta 165, 173-181.

Petrucci, I., Da Pozzo, A., Di Palma, L., 2016. On the ability to electrogenerate hydrogen peroxide and to regenerate ferous ions of three selected carbon-based cathodes for electro-Fenton processes. Chem. Eng. J. 283, 750-758.

Pignatello, J.J., Oliveros, E., Mac Kay, A., 2006. Advanced oxidation processes for organic contaminant destruction based on the Fenton reaction and related chemistry. Crit. Rev. Env. Sci. Tec. 36, 1-84.

Qiang, Z., Chang, J.H., Huang, C.P., 2003. Electrochemical generation of $Fe^{2+}$ in Fenton oxidation processes. Water Res. 37, 1308-1319.

Ramirez, H.J., Costa, C.A., Madeira, L.M., 2005. Experimental design to optimize the degradation of the synthetic dye Orange II using Fenton's reagent. Catal. Today 107-108, 68-76.

Ramirez, J.H., Duarte, F.M., Martins, F.G., Costa, C.A., Madeira, L.M., 2009. Modelling of the synthetic dye Orange II degradation using Fenton's reagent: from batch to continuous reactor operation. Chem. Eng. J. 148, 394-404.

Ré, J.L., De Méo, M.P., Laget, M., Guiraud, H., Castegnaro, M., Vanelle, P., Duménil, G., 1997. Evaluation of the genotoxic activity of metronidazole and dimetriazole in human lymphocytes by the comet assay. Mutat. Res. Fund. Mol. M. 375, 147-155.

Rivera-Utrilla, J., Prados-Joya, G., Sánchez-Polo, M., Ferro-García, M.A., Bautista-Toledo, I., 2009. Removal nitroimidazole antibiotics from aqueous solution by adsorption/bioadsorption on activated carbon. J. Hazard. Mater. 170, 298-305.

Saïdi, I., Soutrel, I., Floner, D., Fourcade, F., N., B., Amrane, A., Geneste, F., 2014. Indirect electroreduction as pretreatment to enhance biodegradability of metronidazole. J. Hazard. Mater. 278, 172-179.

Sánchez-Polo, M., Rivera-Utrilla, J., Prados-Joya, G., Ferro-García, M.A., Bautista-Toledo, I., 2008. Removal of pharmaceutical compounds, nitroimidazoles, from waters by using the ozone/carbon system. Water Res. 42, 4163-4171.

Scott, J.P., Ollis, D.F., 1995. Integration of chemical and biological processes for water treatment: review and recommendations. Environmental Progress 14, 88-103.

Shemer, H., Kunukcu, Y.K., Linden, K.G., 2006. Degradation of the pharmaceutical metronidazole via UV Fenton and photo-Fenton processes. Chemosphere 63, 293-276.

646 Spérandio, M., Paul, E., 2000. Estimation of wastewater biodegradable COD fractions by
647 combining respirometric experiments in various $S_o/X_o$ ratios. Water Res. 34, 1233-1246.
648 Stasinakis, A.S., 2008. Use of selected advanced oxidation processes (AOPs) for wastewater
649 treatment - a mini review. Glob. Nest J. 10, 376-385.
650
651 Sun, S.P., Li, C.J., Sun, J.H., Shib, S.H., Fand, M.H., Zhoua, Q., 2009. Decoloration of an azo
652 dye Orange G in aqueous solution by Fenton oxidation process: effect of system parameters
653 and kinetic study. J. Hazard. Mater. 161, 1052-1057.
654
655 Tally, F.P., Sullivan, C.E., 1981. Metronidazole in vitro activity, pharmacology and efficacy
656 in anaerobic bacterial infections. Pharmacotherapy 1, 28-38.
657
658 Trujillo, D., Font, X., Sánchez, A., 2006. Use of Fenton reaction for the treatment of leachate
659 from composting of different wastes. J. Hazard. Mater. 138, 201-204.
660
661 Vulliet, E., Cren-Olivé, C., 2011. Screening of pharmaceuticals and hormones at the regional
662 scale, in surface and in groundwaters intented to human consumption. Envir. Pollut. 159,
663 2929-2934.
664
665 Yahiat, S., Fourcade, F., Brosillon, S., Amrane, A., 2011. Removal of antibiotics by
666 integrated process coupling photocatalysis and biological treatment - Case of tetracycline and
667 tylosin. Int. Biodeter. Biodegr. 65, 997-1003.
668
669 Zhou, L., Zhou, M., Zhang, C., Jiang, Y., Bi, Z., Yang, J., 2013. Electro-Fenton degradation
670 of p-nitrophenol using the anodized graphite felts. Chem. Eng. J. 233, 185-192.
671
672 Zhou, M., Yu, Q., Lei, L., Barton, G., 2007. Electro-Fenton method for the removal of Methyl
673 Red in an efficient electrochemical system. Sep. Purif. Technol. 57, 380-387.
674
675
676
677
678
679
680
681
682
683
684
685

686

**Figures Legends**

**Figure 1: a)** Time-courses of MTZ degradation (with or without tert-butanol) and its mineralization during electrolysis. Experimental conditions: $C_0$ 100 mg $L^{-1}$, I =0.04 mA $cm^{-2}$, $[Fe^{2+}]$ = 0.1 mM, pH = 3, $[Na_2SO_4]$ =0.05 M. **b)** Current-potential curve obtained with a vitreous carbon rotating electrode (S = 3.2 $10^{-2}$ $cm^2$ and 1500 rpm), r = 5 mV $s^{-1}$, under nitrogen atmosphere and T = 298 K, for 100 mg $L^{-1}$ MTZ (continuous line) at pH 3 in $Na_2SO_4$ 0.1 M (dashed line).

**Figure 2**: Effect of the applied current density on the MTZ degradation **(a)** and its mineralization **(b)**. Experimental conditions: $C_0$ =100 mg $L^{-1}$, $[Fe^{2+}]$ =0.1 mM, pH=3, $Na_2SO_4$=50 mM, V=250 mL.

**Figure 3:** Evolution of MTZ degradation with the electric charge for different current densities **(a)** and effect of the current density on the accumulated $H_2O_2$ production after 1 hour of electrolysis **(b)**. Experimental conditions: $C_0$ =100 mg $L^{-1}$, $[Fe^{2+}]$ =0.1 mM, pH=3, $Na_2SO_4$=50 mM, V=250 mL.

**Figure 4**: **(a)** Effect of the applied current density on the total iron ions concentration. Experimental conditions: $C_0$ =100 mg $L^{-1}$, $[Fe^{2+}]$ =0.1 mM, pH=3, $Na_2SO_4$=50 mM. **(b)** Regeneration of $Fe^{2+}$ at 0.04 and 0.07 mA $cm^{-2}$. Experimental conditions $C_0$ =100 mg $L^{-1}$, $[Fe^{3+}]$ =0.1 mM, pH=3, $Na_2SO_4$=50 mM.

705

706

Table 1 : Apparent kinetic rate constants $K_{app}$ obtained during the EF treatment at various initial MTZ concentrations, Fe (II) concentration, pH and applied current intensity.

| [MTZ] $_{initial}$ (mg L$^{-1}$) | [Fe$^{2+}$] (mM) | Current density (mA cm$^{-2}$) | pH | kapp (min$^{-1}$) |
|---|---|---|---|---|
| 100 | 0.10 | 0.07 | 3 | 0.24 |
| 200 | 0.10 | 0.07 | 3 | 0.06 |
| 300 | 0.10 | 0.07 | 3 | 0.04 |
| 500 | 0.10 | 0.07 | 3 | 0.04 |
| | | | | |
| 100 | 0.10 | 0.04 | 3 | 0.08 |
| 100 | 0.10 | 0.11 | 3 | 0.22 |
| 100 | 0.10 | 0.22 | 3 | 0.23 |
| 100 | 0.10 | 0.45 | 3 | 0.23 |
| | | | | |
| 100 | 0.05 | 0.07 | 3 | 0.15 |
| 100 | 0.5 | 0.07 | 3 | 0.19 |
| 100 | 1.00 | 0.07 | 3 | 0.14 |
| | | | | |
| 100 | 0.10 | 0.07 | 2 | 0.18 |
| 100 | 0.10 | 0.07 | 5 | 0.08 |
| 100 | 0.10 | 0.07 | 7 | 0.08 |
| 100 | 0.10 | 0.07 | 9 | 0.08 |

Table2 : Accumulated hydroxyl radicals production obtained during electro-Fenton treatment at various ferrous ion concentrations and various pH

| [MTZ] $_{initial}$ (mg L$^{-1}$) | [Fe$^{2+}$] (mM) | Current density (mA cm$^{-2}$) | pH | [$^{\bullet}$OH] (mM) |
|---|---|---|---|---|
| 100 | 0.05 | 0.07 | 3 | $1.52 \pm 0.03$ |
| 100 | 0.1 | 0.07 | 3 | $2.28 \pm 0.01$ |
| 100 | 0.5 | 0.07 | 3 | $2.20 \pm 0.03$ |
| 100 | 1.00 | 0.07 | 3 | $1.56 \pm 0.02$ |
| | | | | |
| 100 | 0.10 | 0.07 | 2 | $1.95 \pm 0.09$ |
| 100 | 0.10 | 0.07 | 5 | $0.33 \pm 0.02$ |
| 100 | 0.10 | 0.07 | 7 | $0.29 \pm 0.04$ |
| 100 | 0.10 | 0.07 | 9 | $0.21 \pm 0.02$ |

Table 3: Biodegradability of by-product of MTZ. Experimental Conditions: C0 = 100 mg L$^{-1}$

[Fe$^{2+}$ ] =0.1 mM, Na$_2$SO$_4$=50 mM, V=250 mL , and 0.07 mA cm$^{-2}$ of current density.

| Time (min) | BOD$_5$/COD |
|---|---|
| 0 | 0.01 |
| 30 | 0.24 |
| 60 | 0.46 |
| 90 | 0.46 |
| 120 | 0.70 |
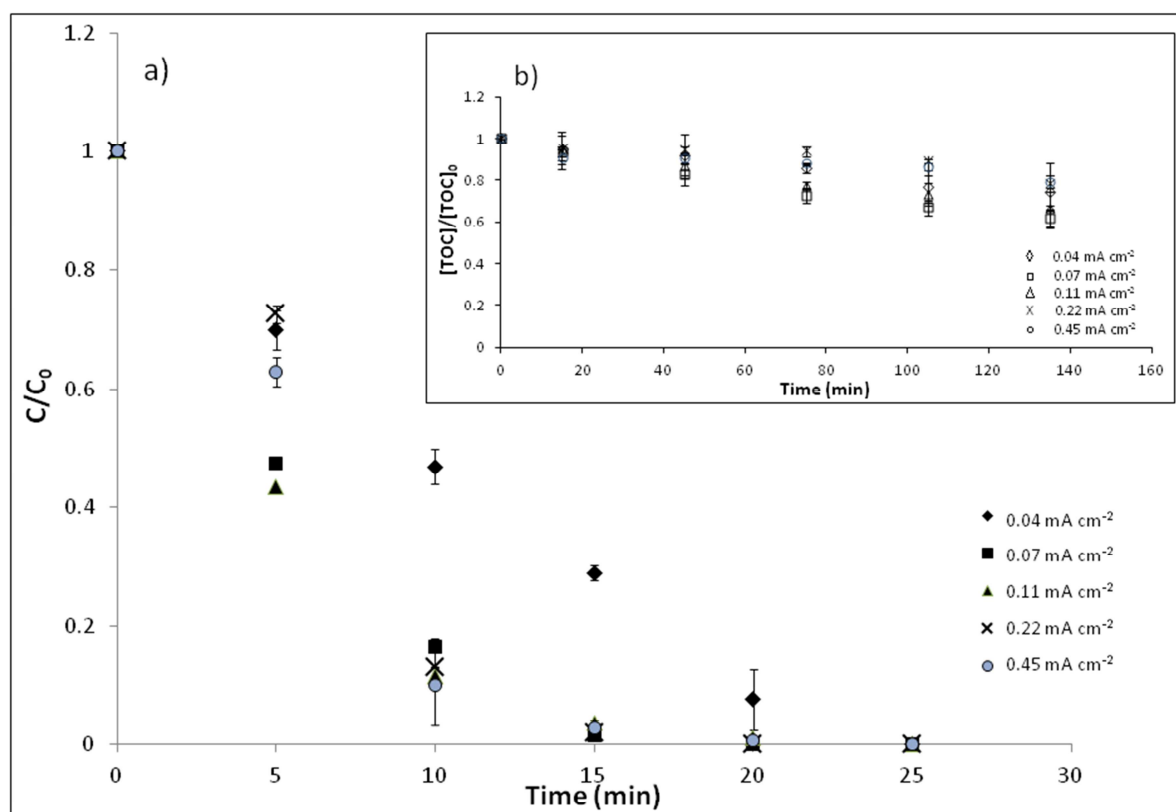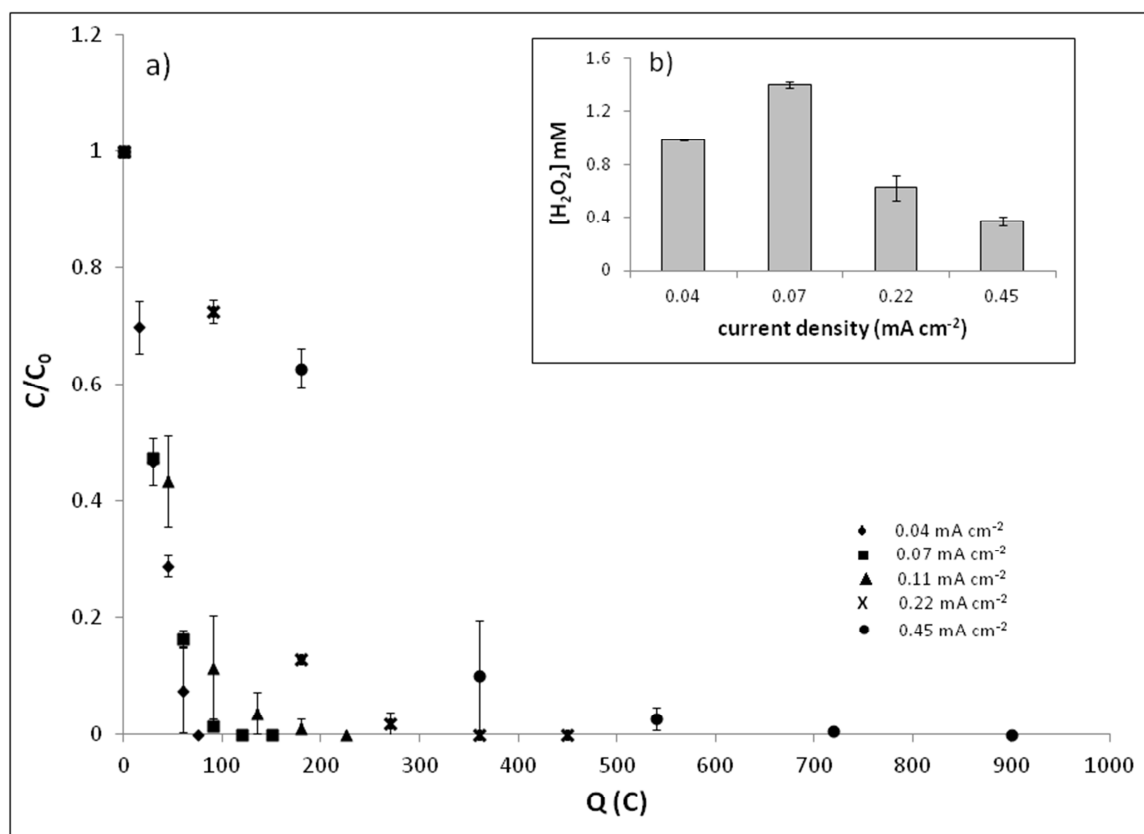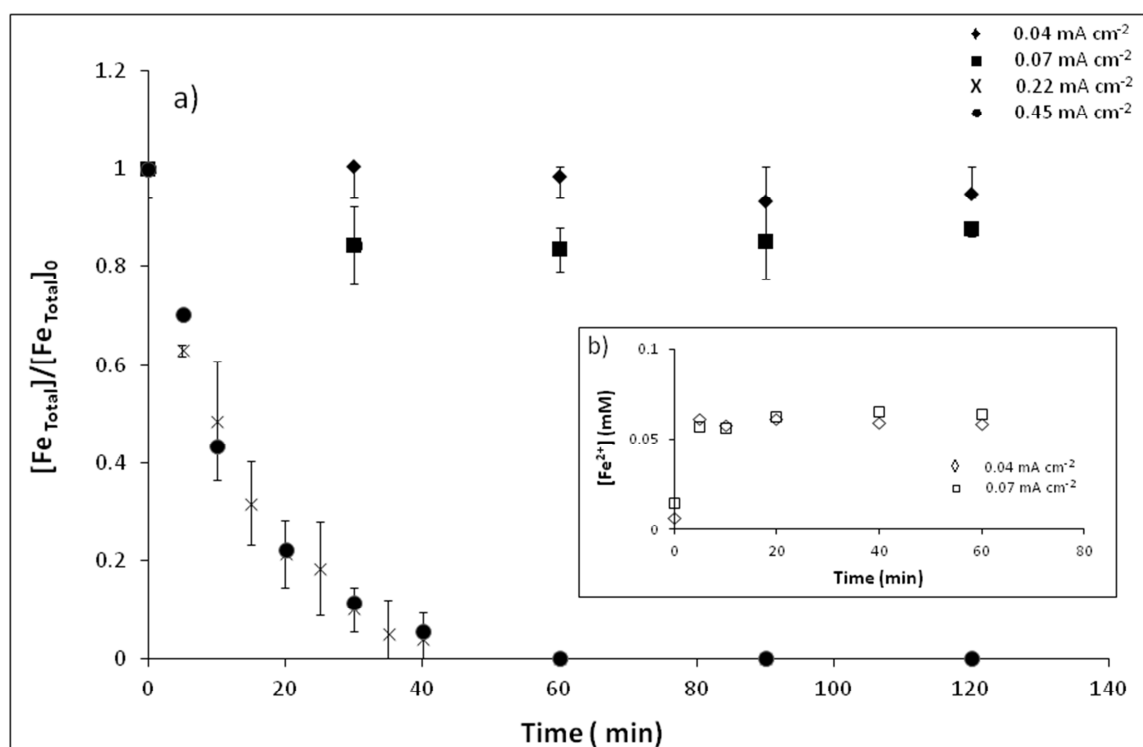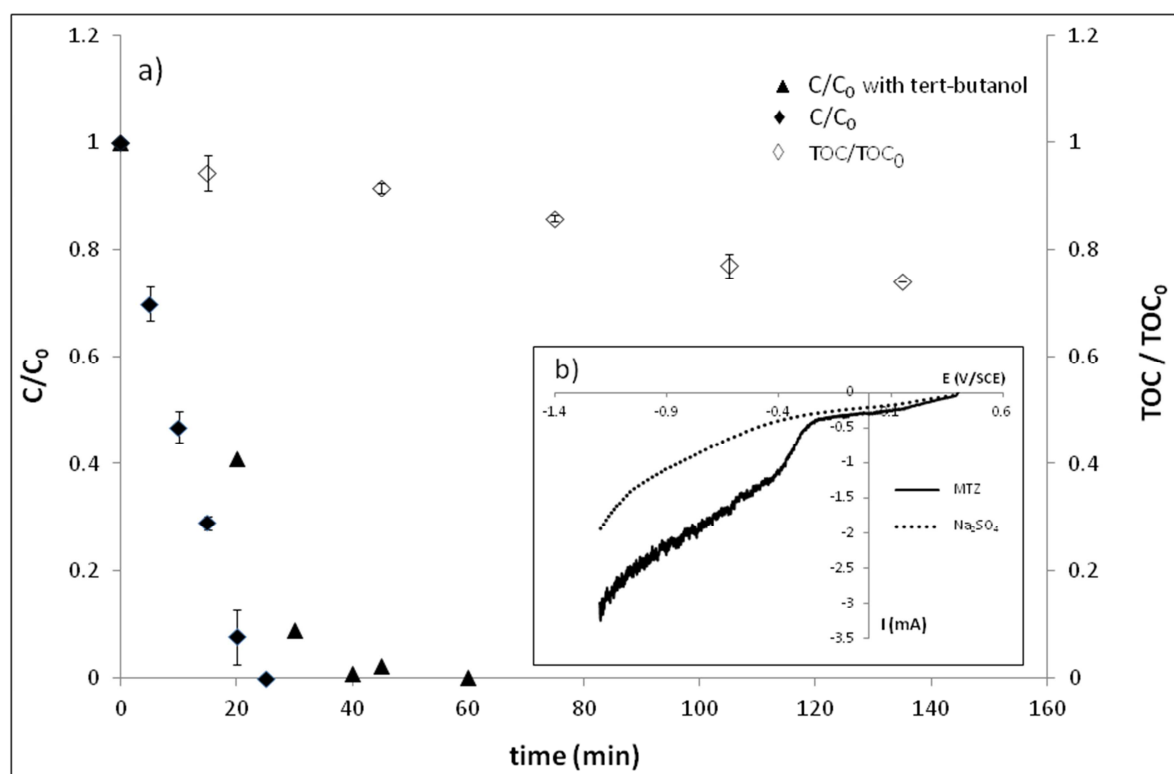
Highlights

- MTZ electroreduction involved in its degradation not in its mineralization
- Good regeneration of ferrous ions up to 0.07 mA.cm$^{-2}$
- Highest $^{\bullet}$OH production for 0.07 mA.cm$^{-2}$, pH 3 and 0.1 mM of ferrous ions
- Limit of biodegradability reached for 60 min of electrolysis according to BOD$_5$ test
- Results from BOD$_5$ reinforced by respirometric study implemented during 21 days